Journal of Controlled Release 370 (2024) 468–478

Contents lists available at ScienceDirect

Journal of Controlled Release

journal homepage: www.elsevier.com/locate/jconrel

Half-life extension *via* ABD-fusion leads to higher tumor uptake of an affibody-drug conjugate compared to PAS- and XTENylation.

Jie Zhang [a,1], Vitalina Bodenko [b,c,1], Maria Larkina [b,d], Ekaterina Bezverkhniaia [b,e], Tianqi Xu [f], Yunqi Liao [f], Ayman Abouzayed [e], Evgenii Plotnikov [b], Maria Tretyakova [b], Feruza Yuldasheva [b], Mikhail V. Belousov [b,d], Anna Orlova [e], Vladimir Tolmachev [f], Torbjörn Gräslund [a,*], Anzhelika Vorobyeva [f,*]

[a] *Department of Protein Science, KTH Royal Institute of Technology, Roslagstullsbacken 21, Stockholm 114 17, Sweden*
[b] *Research Centrum for Oncotheranostics, Research School of Chemistry and Applied Biomedical Sciences, Tomsk Polytechnic University, Tomsk 634050, Russia*
[c] *Scientific and Educational Laboratory of Chemical and Pharmaceutical Research, Siberian State Medical University, Ministry of Health of the Russian Federation, Tomsk 634050, Russia*
[d] *Siberian State Medical University, Ministry of Health of the Russian Federation, Tomsk 634050, Russia*
[e] *Department of Medicinal Chemistry, Uppsala University, 751 23 Uppsala, Sweden*
[f] *Department of Immunology, Genetics and Pathology, Uppsala University, 751 85 Uppsala, Sweden*

A R T I C L E I N F O

Keywords:
Affibody molecule
Albumin binding domain
ABD
HER2
PASylation
XTENylation
DM1
Affibody-drug conjugate
Half-life

A B S T R A C T

A critical parameter during the development of protein therapeutics is to endow them with suitable pharmacokinetic and pharmacodynamic properties. Small protein drugs are quickly eliminated by kidney filtration, and *in vivo* half-life extension is therefore often desired. Here, different half-life extension technologies were studied where PAS polypeptides (PAS300, PAS600), XTEN polypeptides (XTEN288, XTEN576), and an albumin binding domain (ABD) were compared for half-life extension of an anti-human epidermal growth factor receptor 2 (HER2) affibody-drug conjugate. The results showed that extension with the PAS or XTEN polypeptides or the addition of the ABD lowered the affinity for HER2 to some extent but did not negatively affect the cytotoxic potential. The half-lives in mice ranged from 7.3 h for the construct including PAS300 to 11.6 h for the construct including PAS600. The highest absolute tumor uptake was found for the construct including the ABD, which was 60 to 160% higher than the PASylated or XTENylated constructs, even though it did not have the longest half-life (9.0 h). A comparison of the tumor-to-normal-organ ratios showed the best overall performance of the ABD-fused construct. In conclusion, PASylation, XTENylation, and the addition of an ABD are viable strategies for half-life extension of affibody-drug conjugates, with the best performance observed for the construct including the ABD.

1. Introduction

In vivo, proteins smaller than 60–70 kDa are quickly cleared by kidney filtration and consequently have a short half-life in circulation. This is undesirable for many therapeutic applications since a long half-life increases the bioavailability and allows for less frequent drug administration. Different methods to increase the hydrodynamic radius of protein drugs to above the cut-off for kidney filtration have been described, consequently increasing the time in circulation. The methods include PEGylation, XTENylation, PASylation, albumin binding, albumin fusion, Fc-fusion, *etc.* [1]. Some of these, albumin binding, albumin fusion, and Fc-fusion, gain further half-life extension by indirect or direct interaction with the neonatal Fc receptor (FcRn) [2].

For protein-based cancer drugs, the ultimate goal of *in vivo* half-life extension is to increase the absolute tumor accumulation and to optimize the tumor-to-normal-organ uptake. To understand how these parameters correlate with the *in vivo* half-life, we have, in this study, compared different strategies for half-life extension of an affibody-based drug conjugate.

A possibility is to use unstructured amino acid chains, such as PAS and XTEN polypeptides, to increase the hydrodynamic radius. The PAS polypeptide consists of proline, alanine, and serine in a random order

* Corresponding authors.
E-mail addresses: torbjorn@kth.se (T. Gräslund), anzhelika.vorobyeva@igp.uu.se (A. Vorobyeva).
[1] These authors contributed equally to this work

https://doi.org/10.1016/j.jconrel.2024.04.051
Received 23 February 2024; Received in revised form 19 April 2024; Accepted 29 April 2024
Available online 8 May 2024

[3]. It is non-charged and is characterized by high solubility and a large hydrodynamic radius. PASylation has been shown to extend the *in vivo* half-life of many different proteins, even in cases where the molecular weight of the fusion is less than the molecular weight cut-off for kidney filtration [3]. The XTEN polypeptide consists of a random sequence of alanine, proline, serine, threonine, glycine, and glutamic acid, which results in a hydrophilic, negatively charged polymer [4]. The original sequence comprises 864 amino acids, but shorter versions (288 or 576 amino acids) have also been explored for half-life extension [5]. Both the PAS and the XTEN sequences consist of naturally occurring amino acids and are generally considered to be non-immunogenic and biodegradable. Another possibility is to use an albumin-binding domain. It does not usually, by itself, increase the molecular weight to above the cut-off of kidney filtration. Instead, it associates non-covalently with the abundantly present albumin in blood, which increases the size of the formed complex by the size of albumin (66–67 kDa) to exceed the cut-off of kidney filtration.

For drug conjugates, a long *in vivo* half-life increases the bioavailability. However, using a PAS or XTEN polypeptide generates drug conjugates with a large hydrodynamic radius, which might decrease the extravasation rate, leading to reduced tumor accumulation. Furthermore, the differences in biophysical properties between the PAS polypeptide, XTEN polypeptide, and ABD/albumin complex might confer different propensities for uptake in normal organs and tissues. This is important for clinical application of drug conjugates and other protein drugs since off-target uptake may damage normal organs and cause side effects for the patient.

Affibody molecules are small (6–7 kDa), engineered affinity proteins, and variants with strong, sub-nanomolar affinity to several cancer-relevant receptors have been described [6]. One example is affibody molecules binding to the human epidermal growth factor receptor 2 (HER2), a receptor over-expressed in 20–30% of all breast cancers [7,8]. Particularly, the affibody molecule $Z_{HER2:2891}$ [9], with an affinity of 65 pM (K_D value) to HER2 has been used in several pre-clinical studies.

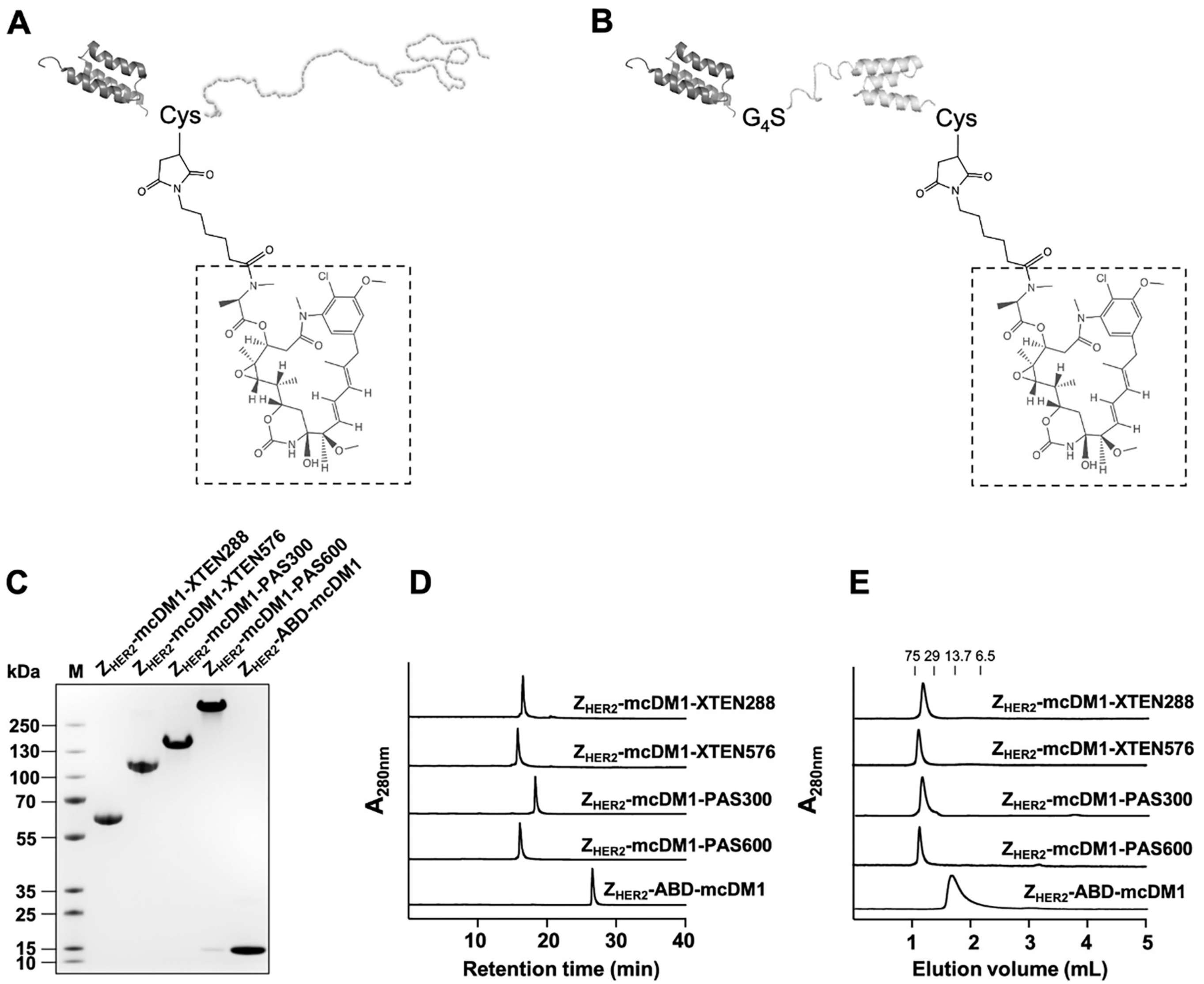

Fig. 1. (A) Schematic representation of the PASylated and the XTENylated affibody drug conjugates consisting of $Z_{HER2:2891}$ (dark grey) followed by a cysteine amino acid with an attached DM1 drug (inside dashed box), and XTEN288, XTEN576, PAS300, or PAS600. (B) Schematic representation of the affibody-ABD drug conjugate, consisting of $Z_{HER2:2891}$ (dark grey) followed by ABD_{035} (light grey) and a C-terminal cysteine with an attached DM1 drug (inside dashed box). A linker with the amino acid sequence Gly-Gly-Gly-Gly-Ser was used to connect the affibody and the ABD. (C) SDS-PAGE analysis of the purified drug conjugates under reducing conditions. The proteins in lane M are marker proteins with their molecular weights indicated to the left of the gel. (D) RP-HPLC analysis of the drug conjugates on a Zorbax SB-C18 column with a linear gradient from 20 to 60% acetonitrile in water supplemented with 0.1% trifluoroacetic acid during 40 min. The flow-rate was 2 mL/min. (E) Size-exclusion chromatography analysis of the conjugates on a Superdex-75 5/150 column, equilibrated and eluted with PBS. The flow rate was 0.45 mL/min. The numbers above the panel indicate the molecular weights (kDa) of standard proteins.

Moreover, radiolabeled HER2-targeting affibody molecules have shown specificity for HER2 in clinical studies, providing high-contrast images, and have been found to be safe in humans [10–13].

Previously, the properties of affibody drug conjugates targeting HER2 have been investigated. They consisted of $Z_{HER2:2891}$ for specific targeting of HER2 over-expressing cells, an albumin binding domain (ABD_{035} [14]) for *in vivo* half-life extension, and different cytotoxic drugs: DM1, MMAE, and MMAF [15,16] attached *via* a maleimidocaproyl (mc) linker to a unique cysteine inserted in the C-terminus of the fusion protein [17–19]. The drugs inhibit tubulin polymerization, and the affibody-drug conjugates containing DM1 or MMAF showed remarkable therapeutic efficacy in xenograft models *in vivo* [16,17]. We found that the drug conjugate, $Z_{HER2:2891}$-ABD_{035}-mcDM1, where mcDM1 represents DM1 connected to a maleimidocaproyl linker, has a half-life in mice of 10.7 h [20].

In this study, the goal was to investigate the properties of affibody drug conjugates including different methods of *in vivo* half-life extension. A series of constructs was designed, including either a PAS polypeptide of 300 or 600 amino acids, an XTEN polypeptide of 288 or 576 amino acids, or an ABD for albumin binding (Fig. 1A, Fig. S1). The PASylated and XTENylated constructs consisted of the HER2 binding affibody molecule $Z_{HER2:2891}$, followed by a cysteine for drug conjugation and XTEN288, XTEN576, PAS300 or PAS600 in the C-terminus. The ABD-containing construct had a slightly different architecture with $Z_{HER2:2891}$ followed by ABD_{035} and ending with a cysteine for DM1 conjugation. All constructs were extended in the N-terminus with the amino acid sequence HEHEHE for purification by immobilized metal-ion affinity chromatography and radiolabeling with technetium-99m tricarbonyl [21,22]. The ABD-containing construct also included three glutamic acids immediately preceding the cysteine, which has previously been found to reduce the hepatic uptake of DM1-containing affibody drug conjugates [18,23]. The binding kinetics, cytotoxic effect, *in vivo* half-life, tumor accumulation, and biodistribution of the drug conjugates were investigated to provide insights into the differences between these half-life extension technologies.

2. Materials and methods

2.1. General

Chemicals were purchased from Thermo Fisher Scientific (Waltham, MA, USA) or Merck (Darmstadt, Germany) unless indicated otherwise in the text. Restriction enzymes were from New England Biolabs (Ipswitch, MA, USA).

2.2. Gene construction

The HER2 binding affibody molecule used in this study was $Z_{HER2:2891}$ [9] herein referred to as Z_{HER2}. The ABD used in this study was ABD_{035} [14]. Genes encoding Z_{HER2}-Cys-XTEN288, Z_{HER2}-Cys-XTEN576, Z_{HER2}-Cys-PAS300, and Z_{HER2}-Cys-PAS600 were synthesized by Thermo Fisher Scientific. The genes had a 5′-sequence encoding the amino acids MHEHEHE. The genes were subcloned into the expression vector pET-26b(+) (Merck Millipore, Burlington, MA, USA) using *Nde*I and *Hind*III restriction enzymes. A cysteine was introduced between $Z_{HER2:2891}$ and the XTEN or PAS polypeptides for site-specific conjugation of mcDM1. The expression plasmid encoding $Z_{HER2:2891}$-ABD-Cys was from a previous study [18]. The gene sequences were confirmed by DNA sequencing.

2.3. Expression and purification of the affibody fusion proteins

The fusion proteins were expressed in *Escherichia coli* BL21 (DE3) Star (New England Biolabs) essentially as described [18]. Over-night cultures (5 mL) were used for inoculation of 500 mL TSBY medium (30 g/L Tryptic soy broth, 5 g/L Yeast extract) supplemented with 50 mg/L kanamycin. The cells were grown at 37 °C until OD_{600} was between 0.5 and 1, at which point protein production was induced by the addition of isopropyl-β-D-1-thiogalactopyranoside (Appolo Scientific, Stockport, UK) to a final concentration of 1 mM. Production was continued overnight, after which the cells were pelleted by centrifugation (6000 ×*g*, 10 min, 4 °C) and stored at −20 °C.

The cell pellets from the production of the PASylated and XTENylated fusion proteins were thawed and resuspended in 20 mL Binding buffer (20 mM sodium phosphate, 0.5 M NaCl, 20 mM imidazole, pH 7.4). The cells were broken by sonication, followed by centrifugation (20,000 ×*g*, 20 min, 4 °C), and the supernatant was collected. The supernatant was further clarified by filtering through a 0.45 μm Acrodisc syringe filter (Pall, Port Washington, NY, USA). The fusion proteins were then purified from the supernatant by Immobilized Metal-Ion Affinity Chromatography (IMAC) on a 1 mL HisTrap FF column (GE Healthcare, Uppsala, Sweden) according to the manufacturer's protocol. Eluted fractions from the IMAC column were further purified by reversed-phase high-performance liquid chromatography (RP-HPLC) using a 20 to 60% gradient of acetonitrile in water with 0.1% trifluoroacetic acid on a Zorbax C18 SB column (Agilent, Santa Clara, CA, USA). Eluted material was pooled, lyophilized, and stored at −20 °C.

The ABD-containing fusion protein was produced and purified as previously described [18]. The cell pellet from expression of $Z_{HER2:2891}$-ABD-Cys was thawed and resuspended in TST-buffer (25 mM Tris, 1 mM EDTA, 200 mM NaCl, 0.05% Tween-20, pH 8.0). The cells were broken by sonication, followed by centrifugation and filtration as described above for the PASylated and XTENylated fusion proteins. $Z_{HER2:2891}$-ABD-Cys, in the supernatant, was purified by affinity chromatography on a HiTrap NHS sepharose column (GE Healthcare) with immobilized HSA. The column was equilibrated with TST after which the supernatant was loaded, followed by extensive washing of the column with TST. The column was washed with 5 mM ammonium acetate (pH 5.5) and bound proteins were eluted with 0.5 M acetic acid (pH 2.3). Eluted fractions were collected, lyophilized, and stored at −20 °C.

2.4. Conjugation with DM1

The lyophilized proteins were redissolved to a concentration of 0.1 mM in PBS (pH 6.5). To reduce potentially oxidized cysteines in the fusion proteins, they were incubated with 5 mM tris (2-carboxyethyl) phosphine (TCEP) for 1 h at 37 °C. The solutions were desalted on PD-10 columns to remove excess TCEP. A freshly prepared solution of mcDM1 (20 mM in DMSO; Levena Biopharma, San Diego), was added at a molar ratio of 2:1 (mcDM1: protein). The mixture was incubated overnight at room temperature. On the following morning, HPLC buffer A (0.1% trifluoroacetic acid in H_2O) was added to the mixture, and the mixture was loaded on a Zorbax SB-C18 column (Agilent, Santa Clara, CA, USA). The drug conjugates were eluted with a linear acetonitrile gradient from 20% to 60% during 40 min. The flowrate was 2 mL/min. The fractions containing eluted drug conjugates were pooled and lyophilized.

2.5. Analysis of HER2 affinity

Surface plasmon resonance (SPR) was used to measure the affinity between the constructs and HER2 using a Biacore T200 instrument (Cytiva, Uppsala, Sweden). One flow cell on a CM5 chip was coated with the extracellular domain of human HER2 (Sino Biological, Beijing, China) in sodium acetate buffer (pH 4.5). Dilution series of the drug conjugates were serially injected over the HER2 surface in duplicates. The chip surface was regenerated with 20 mM HCl for 30 s between injections. The kinetic constants were derived from the sensorgrams using the Biacore T200 Evaluation Software, assuming a 1:1 L interaction model.

2.6. Cell culture

The HER2 positive cell lines SKOV3, SKBR3, AU565, BT474, and the HER2 negative cell lines A549, MCF7, and Ramos were obtained from ATCC (American Type Culture Collection, Manassas, VA, USA) and were cultured according to the supplier's recommendations. All media were supplemented with 1% penicillin-streptomycin (Biowest, Riverside, MO, USA) and 10% FBS.

2.7. In vitro cytotoxicity analysis

The cytotoxicity of the drug conjugates to HER2 positive and negative cells was assessed using a Cell Counting kit-8 (CCK-8, Sigma-Aldrich). Cells were seeded in 96-well plates at a density of 5000 cells/well (2000 cells/well for the SKOV3 cell line) in 100 μL medium, followed by incubation for 24 h to allow the cells to attach. The medium was then changed to a medium containing the drug conjugates at different concentrations, followed by incubation for 3 days. The medium was then aspirated, and cell viability was measured according to the manufacturer's instructions. The dose-response curves were drawn, and the IC_{50} values were determined by Prism (Graphpad Software, La Jolla, CA, USA).

2.8. Radiolabeling of affibody-drug conjugates

The drug conjugates carried a His-Glu-His-Glu-His-Glu peptide sequence ($(HE)_3$-tag) at the N-terminus, which was used for radiolabeling with technetium-99m tricarbonyl following a previously published protocol [18]. The radiolabel stability was evaluated by incubating the purified affibody-drug conjugates with a 1000-fold molar excess of histidine in PBS or with only PBS (control samples) for 4 h at 37 °C. The radiochemical yield and purity were determined by instant thin-layer chromatography (iTLC) eluted with PBS. The iTLC analysis was performed using CR35 BIO Plus Storage Phosphor System and AIDA image analysis software (both from ElysiaRaytest, Bietigheim-Bissingen, Germany).

2.9. Binding specificity, cellular internalization, and binding kinetics of the [^{99m}Tc]Tc-labeled affibody-drug conjugates

HER2-specific binding of the [^{99m}Tc]Tc-labeled drug conjugates to HER2-expressing cells was investigated according to a method described earlier and was performed in triplicates [24]. The binding and internalization rate of the [^{99m}Tc]Tc-labeled drug conjugates by HER2-expressing SKOV3 and BT474 cells were studied using an "acid wash" method described previously and was performed in triplicates [24]. The interaction between [^{99m}Tc]Tc-labeled affibody-drug conjugates and HER2-expressing SKOV3 cells was measured in real-time on a LigandTracer instrument following a previously described method and was performed in triplicates [18]. The obtained data were corrected for radionuclide decay and analyzed using the TraceDrawer software (Ridgeview Instruments, Vänge, Sweden) to determine the equilibrium dissociation constants (K_D) of the interactions. The data underwent an Interaction Map analysis (Ridgeview Diagnostics, Uppsala, Sweden) to assess the heterogeneity of the interactions.

2.10. Animal studies

The animal experiments in CD-1 mice were carried out in agreement with the national guidelines of the Russian Federation for the care and use of the animals. The animal study protocol was approved by the Ethics Committee of the Siberian State Medical University, Tomsk, Russia (protocol code 7715, 20190826). The animal experiments in BALB/c nu/nu mice were carried out in agreement with the Swedish legislation on animal welfare and were approved by the Animal Research Committee at Uppsala University (permit 5.8.18–11,931/2020, approved 28 August 2020).

2.11. Biodistribution studies in CD-1 mice

To study the biodistribution of the [^{99m}Tc]Tc-labeled affibody-drug conjugates, sixty female CD-1 mice were divided into fifteen groups of four mice each. The average mice weight was 29.6 ± 3.5 g. The mice were injected intravenously with 200 pmoles (7 μg for Z_{HER2}-mcDM1-XTEN288 and Z_{HER2}-mcDM1-PAS300; 12.5 μg for Z_{HER2}-mcDM1-XTEN576 and Z_{HER2}-mcDM1-PAS600; 3 μg for Z_{HER2}-ABD-mcDM1; 60 kBq for 4 h, 640 kBq for 24 h, 10240 kBq for 48 h) of the corresponding [^{99m}Tc]Tc-labeled affibody-drug conjugate in 100 μL PBS, containing 1% BSA. After 4, 24, and 48 h, groups of mice were anesthetized and sacrificed by cervical dislocation. The blood, organs, and tissues of interest were collected and weighed, and the activity was measured using an automatic gamma-spectrometer. The activity in blood, calculated as percent of injected dose per gram of blood sample (%ID/g), at 4, 24, and 48 h p.i., was analyzed using Prism (one phase decay model; Graphpad software, La Jolla, CA, USA) for calculation of half-lives.

2.12. Biodistribution studies in tumor-bearing BALB/c nu/nu mice

To study the tumor-targeting properties of the [^{99m}Tc]Tc-labeled affibody-drug conjugates, forty female BALB/c nu/nu mice were implanted subcutaneously in a hind leg with either HER2-expressing SKOV3 cells (10×10^6 cells) or HER2-negative Ramos cells (5×10^6 cells). Two weeks after the implantation, the mice were randomized into nine groups with four mice each. The average mouse weight was 18.4 ± 1.2 g, the average SKOV3 tumor weight was 0.33 ± 0.14 g, and the average Ramos tumor weight was 0.56 ± 0.24 g. The mice were injected intravenously with 200 pmoles (7 μg for Z_{HER2}-mcDM1-XTEN288 and Z_{HER2}-mcDM1-PAS300; 12.5 μg for Z_{HER2}-mcDM1-XTEN576 and Z_{HER2}-mcDM1-PAS600; 3 μg for Z_{HER2}-ABD-mcDM1; 10,240 kBq) of the corresponding [^{99m}Tc]Tc-labeled affibody-drug conjugate in 100 μL PBS, containing 1% BSA. The biodistribution was determined after 48 h, as described above.

2.13. Statistical analysis

Statistical analysis was carried out using Prism. Unpaired *t*-tests were used for the comparison of two values. For the comparison of more than two values, one-way ANOVA with Bonferroni's correction was used.

3. Results

3.1. Production and biochemical characterization of the affibody-drug conjugates

The fusion proteins containing an ABD, a PAS polypeptide, or an XTEN polypeptide were produced in *Escherichia coli,* followed by purification by column chromatography. DM1 was site-specifically attached through a maleimidocaproyl (mc) linker to the unique cysteine residue in each fusion protein, followed by RP-HPLC purification to yield the final drug conjugates. SDS-PAGE analysis (Fig. 1C) confirmed a high purity of the conjugates. The XTENylated and the PASylated conjugates migrated more slowly through the gel than expected from their molecular weights. The drug conjugates were also analyzed by RP-HPLC (Fig. 1D), and a calculation of the area under the curve showed that the purities were above 99%. Z_{HER2}-ABD-mcDM1 was eluted later than the PAS- and XTENylated constructs, indicating a more hydrophobic character. Analysis by size exclusion chromatography under native conditions (Fig. 1E) showed that all five conjugates were eluted as single peaks, indicating no formation of multimers or the presence of degradation products. The XTENylated and the PASylated conjugates were eluted earlier than expected from their molecular weight. Mass spectrometry analysis (Fig. S2) showed that the drug conjugates had the expected molecular weights.

3.2. Evaluation of binding kinetics by surface plasmon resonance analysis

The binding kinetics of the drug conjugates to the extracellular domain of HER2 were determined by surface plasmon resonance analysis, and the results are shown in Table 1, and Fig. S3. The association rates (k_a) of the two PASylated conjugates and the ABD fused conjugate were similar and ranged from 2.6 × 10^5 1/Ms. to 3.7 × 10^5 1/Ms. The association rates for Z_{HER2}-mcDM1-XTEN288 and Z_{HER2}-mcDM1-XTEN576 conjugates were slower, 6.1 × 10^4 1/Ms. and 9.1 × 10^4 1/Ms., respectively. The dissociation rates (k_d) were similar for the five conjugates. The equilibrium dissociation constants (K_D) of the two PASylated conjugates and the ABD-fused conjugate were similar and stronger than the XTENylated conjugates (Table 1). Compared to Z_{HER2}-mcDM1, which was analyzed previously [17], the on-rates were slower for all five constructs, and consequently, the affinities were weaker.

3.3. Cytotoxicity analysis

The cytotoxicity of the XTENylated, PASylated, and ABD-fused drug conjugates was investigated in cell lines with various levels of HER2 expression. On the HER2-positive cell lines (SKOV3, AU565, SKBR3), all conjugates showed dose-dependent cytotoxicity (Fig. 2, Table 2). For the SKOV3 cell line, there was no significant difference among the IC_{50} values, which ranged from 26 nM to 43 nM. For the AU565 cell line, the values ranged from 0.6 nM to 2.6 nM, with the strongest effect for Z_{HER2}-mcDM1-PAS600 and Z_{HER2}-ABD-mcDM1. For the SKBR3 cell line, the IC_{50} value of Z_{HER2}-ABD-mcDM1 was significantly stronger (0.7 nM) than the other four constructs (4.1 nM to 9.6 nM). The curves for the XTENylated and the PASylated drug conjugates had a different shape than the curve for Z_{HER2}-ABD-mcDM1 on the SKBR3 cell line, with a shallower slope around the IC_{50} value. The cytotoxicities of the five constructs were similar to the cytotoxicity of Z_{HER2}-mcDM1, measured in a previous study [17], to the AU565 and SKBR-3 cell lines. In contrast, Z_{HER2}-mcDM1 had a >10-fold stronger cytotoxicity to the SKOV3 cell line compared to the five constructs in this study. On the HER2-negative cell lines, A549 and MCF7, no cytotoxic effect was detected for any of the drug conjugates at the concentrations tested except for a minor effect of the highest concentration of Z_{HER2}-mcDM1-PAS300 and Z_{HER2}-mcDM1-PAS600.

3.4. Radiolabeling of the affibody-drug conjugates

For quantitative analysis of the binding properties, internalization, and biodistribution of the drug conjugates, they were site-specifically labeled with technetium-99m tricarbonyl on the histidine-glutamate $(HE)_3$ amino acid sequence at the N-terminus. A radiochemical purity of over 96% was obtained for all conjugates after purification (Table S1). The results of a radiolabel stability test showed a minor release of 4% for the PAS600 conjugate in histidine and no significant label release for the other conjugates, confirming robust radiolabeling (Table S1).

Table 1
The derived kinetic constants and equilibrium dissociation constants of the interactions between the drug conjugates and HER2.

Analytes	k_a (1/Ms)	k_d (1/s)	K_D (M)
Z_{HER2}-mcDM1-XTEN288	9.1 × 10^4	2.7 × 10^{-4}	3.0 × 10^{-9}
Z_{HER2}-mcDM1-XTEN576	6.1 × 10^4	3.0 × 10^{-4}	4.9 × 10^{-9}
Z_{HER2}-mcDM1-PAS300	3.7 × 10^5	2.8 × 10^{-4}	7.6 × 10^{-10}
Z_{HER2}-mcDM1-PAS600	2.8 × 10^5	1.7 × 10^{-4}	5.9 × 10^{-10}
Z_{HER2}-ABD-mcDM1	2.6 × 10^5	1.8 × 10^{-4}	7.0 × 10^{-10}
Z_{HER2}-mcDM1*	1.6 × 10^6	2.2 × 10^{-4}	1.4 × 10^{-10}

* Historical values for comparison [17].

3.5. Binding specificity, cellular internalization, and affinity to SKOV3 cells of the [^{99m}Tc]Tc-labeled affibody-drug conjugates

The binding specificity of the [^{99m}Tc]Tc-labeled affibody-drug conjugates containing a PAS or XTEN polypeptide extension was evaluated using the HER2-expressing SKOV3 and BT474 cell lines (Fig. 3). For all conjugates, the cell-associated activity was significantly lower in the presence of a large excess of the corresponding non-radiolabeled affibody-drug conjugate compared to the cells incubated with [^{99m}Tc]Tc-labeled affibody-drug conjugate only, showing that the interaction with the cells was HER2 specific. The binding specificity of [^{99m}Tc]Tc-Z_{HER2}-ABD-mcDM1 has been demonstrated previously in an analogous experiment [19].

The internalization rate of the [^{99m}Tc]Tc-labeled affibody-drug conjugates by HER2-expressing SKOV3 and BT474 cells was studied by continuously incubating the cells with the conjugates for 24 h. All conjugates had a rapid association with the cells, reaching a plateau at 4–6 h. The values for the internalized fraction were similar among the conjugates, being on average 28% to 35% in SKOV3 cells and 22% to 28% in BT474 cells at the 24 h time point (Fig. 4, Fig. S4).

The interaction between the [^{99m}Tc]Tc-labeled affibody-drug conjugates and living SKOV3 cells was measured in real-time (Table 3, Fig. S5). The interaction of all conjugates was characterized by rapid association and slow dissociation. The analysis of the interactions using InteractionMap showed two interactions of similar weight, one with a stronger affinity (in the sub-nanomolar to the low nanomolar range) and one with a weaker affinity (nanomolar range), for the PASylated and XTENylated conjugates. Two interactions were also observed for [^{99m}Tc]Tc-Z_{HER2}-ABD-mcDM1, however, the contribution of the high-affinity interaction (K_{D1}) was twice higher (approx. 65%) compared to the PASylated and XTENylated conjugates (*ca.* 30% to 40%).

3.6. Biodistribution in CD-1 mice

To study and compare the biodistribution of the [^{99m}Tc]Tc-labeled affibody-drug conjugates over time, they were injected intravenously in CD-1 mice, and the activity in organs and tissues was measured at 4 h, 24 h, and 48 h after injection (Fig. 5).

All conjugates had prolonged retention in blood compared to the parental Z_{HER2} affibody molecule, which is rapidly excreted from blood with only 2.0 ± 0.2 %ID/g present 30 min after injection [25]. [^{99m}Tc]Tc-Z_{HER2}-mcDM1-PAS300 and [^{99m}Tc]Tc-Z_{HER2}-mcDM1-XTEN288 had the shortest half-life (7.3 and 7.6 h, respectively), followed by [^{99m}Tc]Tc-Z_{HER2}-mcDM1-XTEN576 (8.7 h) and [^{99m}Tc]Tc-Z_{HER2}-ABD-mcDM1 (9.0 h). The longest half-life of 11.6 h was observed for [^{99m}Tc]Tc-Z_{HER2}-mcDM1-PAS600. The uptake in the liver was relatively low at all studied time points, and the area-under-the-curve (AUC) values for the XTENylated and PASylated conjugates were lower or similar to the AUC-value for [^{99m}Tc]Tc-Z_{HER2}-ABD-mcDM1.

The uptake in all normal organs followed the blood kinetics, i. e., when the blood concentration decreased over time, so did the uptake in normal organs. The only exception was the uptake of [^{99m}Tc]Tc-Z_{HER2}-ABD-mcDM1 in bone, where the uptake was relatively steady over the 48 h of the experiment. The uptake in the small intestine was lower for the smaller constructs [^{99m}Tc]Tc-Z_{HER2}-mcDM1-PAS300, [^{99m}Tc]Tc-Z_{HER2}-mcDM1-XTEN288, and [^{99m}Tc]Tc-Z_{HER2}-ABD-mcDM1.

The kidney was the organ with the highest uptake of activity, which indicated renal excretion for all conjugates. At 4 h and 24 h p.i. the conjugates with the larger molecular weight, [^{99m}Tc]Tc-Z_{HER2}-mcDM1-XTEN576 and [^{99m}Tc]Tc-Z_{HER2}-mcDM1-PAS600, had lower uptake in kidneys than [^{99m}Tc]Tc-Z_{HER2}-mcDM1-XTEN288, [^{99m}Tc]Tc-Z_{HER2}-mcDM1-PAS300 and [^{99m}Tc]Tc-Z_{HER2}-ABD-mcDM1, resulting in *ca.* two-fold smaller AUC-values (Fig. 5). The AUC-values for [^{99m}Tc]Tc-Z_{HER2}-mcDM1-XTEN288 and [^{99m}Tc]Tc-Z_{HER2}-mcDM1-PAS300 were comparable with the AUC value for [^{99m}Tc]Tc-Z_{HER2}-ABD-mcDM1. The activity uptake in other organs and tissues decreased over time. Overall,

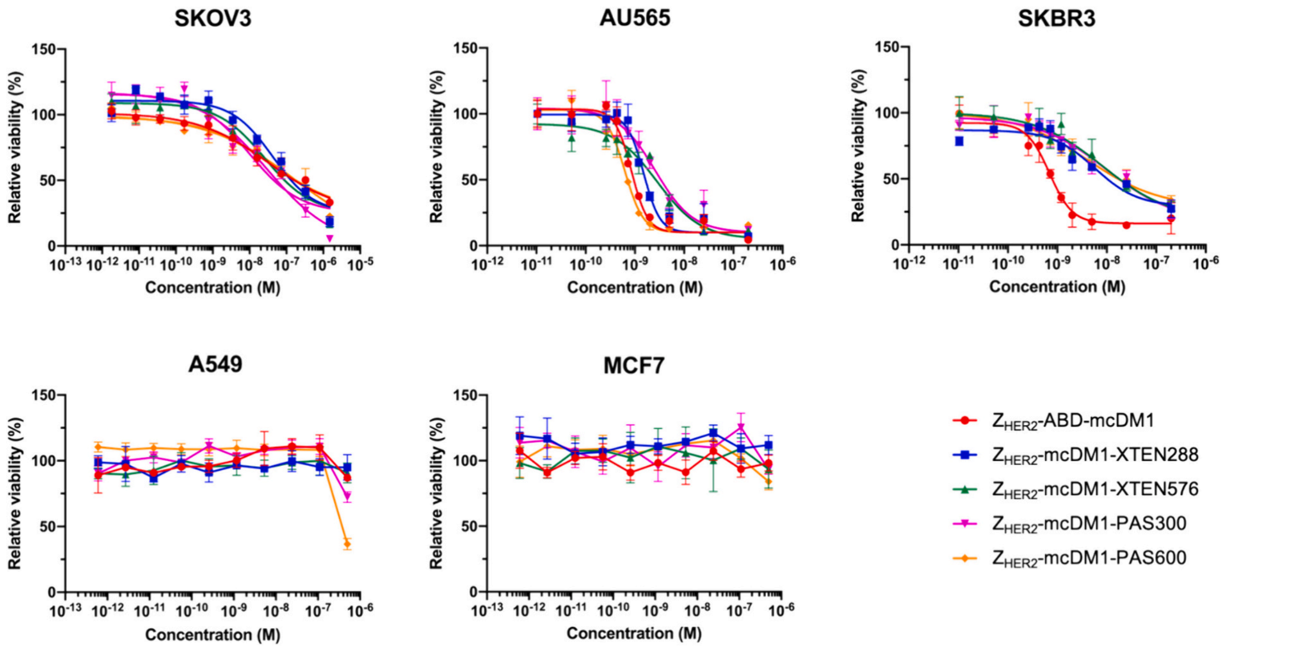

Fig. 2. Cytotoxic effect of the drug conjugates. The cells were incubated with different concentrations of the drug conjugates for 3 d before determination of viability. All values were normalized to cells grown without drug conjugate, which was set to 100%. The experiment was performed in quadruplicates, and the mean is displayed with error bars corresponding to 1 SD.

Table 2
Cytotoxicity of the affibody drug conjugates.

Cell Line	IC$_{50}$ (nM)		
	SKOV3	AU565	SKBR-3
Z$_{HER2}$-mcDM1-XTEN288	43	1.5	5.7
Z$_{HER2}$-mcDM1-XTEN576	26	2.8	8.3
Z$_{HER2}$-mcDM1-PAS300	30	2.6	9.6
Z$_{HER2}$-mcDM1-PAS600	41	0.6	4.1
Z$_{HER2}$-ABD-mcDM1	34	0.8	0.7
Z$_{HER2}$-mcDM1*	1.9	0.3	0.3

* Historical values for comparison [17].

[^{99m}Tc]Tc-Z$_{HER2}$-mcDM1-XTEN576 and [^{99m}Tc]Tc-Z$_{HER2}$-mcDM1-PAS600 were excreted slower from the body than the other conjugates, having higher activity in the rest of carcass at 4 h p.i., however, at 24 h and 48 h p.i. their retention was similar to [^{99m}Tc]Tc-Z$_{HER2}$-ABD-mcDM1.

3.7. Biodistribution in tumor-bearing BALB/c nu/nu mice

To study the specificity of tumor targeting, the tumor uptake of [^{99m}Tc]Tc-labeled affibody-drug conjugates in BALB/c nu/nu mice bearing HER2-expressing [26] SKOV3 xenografts was compared to the tumor uptake in mice bearing HER2-negative Ramos xenografts. At 48 h p.i., the uptake of the XTENylated and PASylated conjugates in SKOV3 xenografts was significantly higher than in the Ramos xenografts (Fig. 6A). The average values of uptake in the Ramos xenografts were below 0.5 %ID/g for the conjugates with lower hydrodynamic radius, [^{99m}Tc]Tc-Z$_{HER2}$-mcDM1-XTEN288 and [^{99m}Tc]Tc-Z$_{HER2}$-mcDM1-PAS300, and below 2 %ID/g for [^{99m}Tc]Tc-Z$_{HER2}$-mcDM1-XTEN576, [^{99m}Tc]Tc-Z$_{HER2}$-mcDM1-PAS600, and around 1 %ID/g for [^{99m}Tc]Tc-Z$_{HER2}$-ABD-mcDM1. To compare the tumor targeting specificity among the conjugates, the tumor specificity uptake index was calculated by dividing the value of uptake (%ID/g) of a conjugate in HER2-expressing SKOV3 xenografts by the value of its uptake in HER2-negative Ramos xenografts (Fig. 6B). [^{99m}Tc]Tc-Z$_{HER2}$-mcDM1-XTEN288 and [^{99m}Tc]Tc-Z$_{HER2}$-ABD-mcDM1 had the same specificity indexes, which were also

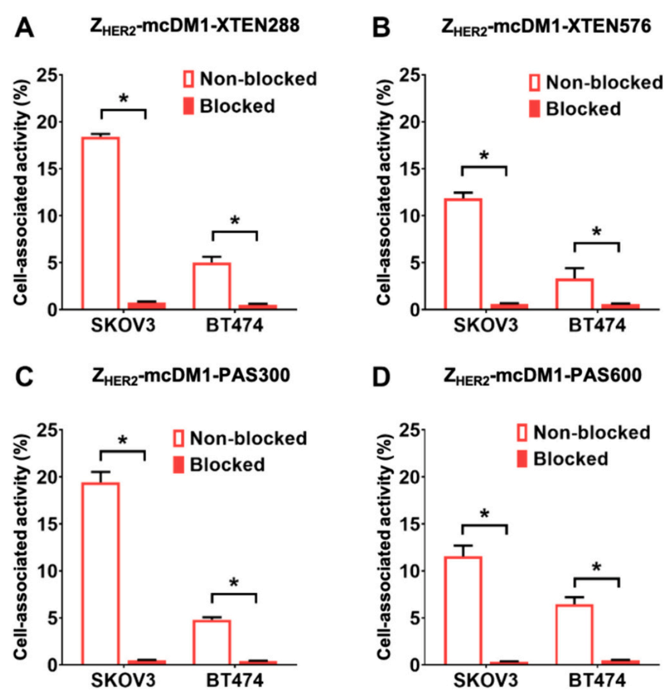

Fig. 3. HER2-binding specificity of the [^{99m}Tc]Tc-labeled affibody-drug conjugates. The HER2-expressing SKOV3 and BT474 cells were incubated with the corresponding non-labeled affibody-drug conjugate (1000 nM) before incubation with the [^{99m}Tc]Tc-labeled affibody-drug conjugate (2 nM). The values are an average of three samples ±1 SD. The asterisks indicate a statistically significant difference between the non-blocked and blocked groups.

the highest, followed by [^{99m}Tc]Tc-Z$_{HER2}$-mcDM1-PAS300 and [^{99m}Tc]Tc-Z$_{HER2}$-mcDM1-XTEN576 having the same index, and [^{99m}Tc]Tc-Z$_{HER2}$-mcDM1-PAS600 had the lowest index.

The comparison of uptake in SKOV3 xenografts among the conjugates 48 h p.i. showed that [^{99m}Tc]Tc-Z$_{HER2}$-ABD-mcDM1 provided a

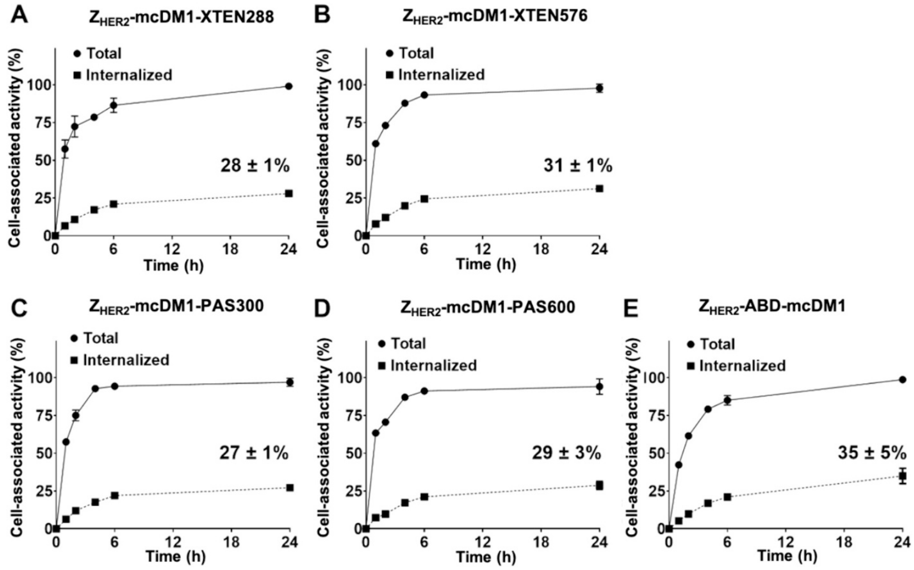

Fig. 4. Binding and internalization rate of the [^{99m}Tc]Tc-labeled affibody-drug conjugates in SKOV3 cells during continuous incubation for 24 h. Data are shown as the average ± 1 SD and are normalized to the maximal value of cell-associated activity (100%). The numbers in the panels correspond to the internalized fraction at the 24-h time point ±1 SD.

Table 3
Equilibrium dissociation constants for high affinity (K_{D1}) and lower affinity (K_{D2}) interactions between [^{99m}Tc]Tc-labeled affibody-drug conjugates and living SKOV3 cells. The values are an average of three independent experiments ±1 SD.

Drug conjugate	K_{D1} (nM)	Weight (%)	K_{D2} (nM)	Weight (%)
[^{99m}Tc]Tc-Z_{HER2}-mcDM1-XTEN288	1.0 ± 0.2	42 ± 1	18.9 ± 1.4	40 ± 0
[^{99m}Tc]Tc-Z_{HER2}-mcDM1-XTEN576	0.70 ± 0.05	35 ± 3	20.1 ± 1.5	47 ± 2
[^{99m}Tc]Tc-Z_{HER2}-mcDM1-PAS300	0.37 ± 0.06	40 ± 2	10.0 ± 1.6	41 ± 2
[^{99m}Tc]Tc-Z_{HER2}-mcDM1-PAS600	0.16 ± 0.02	36 ± 3	7.0 ± 0.5	48 ± 4
[^{99m}Tc]Tc-Z_{HER2}-ABD-mcDM1	0.46 ± 0.14	64 ± 2	29.7 ± 2.7	20 ± 4

significantly higher tumor uptake (8.8 ± 1.2 %ID/g) than the other conjugates (Fig. 6). The uptake of [^{99m}Tc]Tc-Z_{HER2}-mcDM1-PAS600 was significantly higher than that of [^{99m}Tc]Tc-Z_{HER2}-mcDM1-PAS300 (5.6 ± 1.1 %ID/g *vs.* 3.3 ± 0.3 %ID/g). There were no significant differences between the uptake of [^{99m}Tc]Tc-Z_{HER2}-mcDM1-XTEN288, [^{99m}Tc]Tc-Z_{HER2}-mcDM1-XTEN576, and [^{99m}Tc]Tc-Z_{HER2}-mcDM1-PAS300 in the SKOV3 xenografts.

When comparing the biodistribution of the [^{99m}Tc]Tc-labeled affibody-drug conjugates in CD-1 mice and BALB/c nu/nu mice bearing SKOV3 xenografts at 48 h (Fig. S6), a similar pattern of uptake was observed across the majority of normal organs and tissues. This suggests a reasonable correlation in biodistribution while considering the variations in mouse size and strains.

To compare the efficiency of drug delivery to the tumor *versus* the uptake in normal organs and tissues, the uptake in the tumor was divided by the uptake in normal organs or tissues to provide tumor-to-organ ratios (Fig. S7). The tumor-to-organ ratios of [^{99m}Tc]Tc-Z_{HER2}-mcDM1-XTEN576 and [^{99m}Tc]Tc-Z_{HER2}-mcDM1-PAS600 were similar. Overall, [^{99m}Tc]Tc-Z_{HER2}-mcDM1-XTEN288 and [^{99m}Tc]Tc-Z_{HER2}-ABD-mcDM1 provided the highest tumor-to-organ ratios (except tumor-to-kidneys) among all conjugates. Compared to [^{99m}Tc]Tc-Z_{HER2}-mcDM1-XTEN288, [^{99m}Tc]Tc-Z_{HER2}-ABD-mcDM1 provided significantly higher tumor-to-spleen, tumor-to-kidneys, tumor-to-pancreas, and tumor-to-bone ratios, while for the other organs and tissues, the difference between these two conjugates was not statistically significant.

4. Discussion

Half-life extension is often desirable for small protein drugs to provide them with optimal pharmacokinetic properties. For oncology applications, this includes a high absolute uptake in the tumor, and low uptake in normal organs resulting in high tumor-to-normal-organ ratios. In this study, we investigated different half-life extension technologies in the context of a HER2-specific affibody-drug conjugate. The aim was to understand the differences conferred by PASylation, XTENylation, and ABD-fusion.

The mass spectrometry analysis showed the expected molecular weights for both PASylated and XTENylated constructs, while the SDS-PAGE analysis indicated much higher molecular weights due to their slow migration through the gel. Earlier studies have shown the same phenomenon, and it was suggested that the hydrophilic PAS and XTEN polypeptides do not bind SDS efficiently and, therefore, migrate more slowly through the gel [3,4]. The migration rate could also be affected by the differences in structural shape (globular *vs.* unstructured) and inherent charge of the polypeptide, and our result shows that the PASylated constructs migrate more slowly than the XTENylated constructs, where the latter is inherently negatively charged and should therefore migrate faster through the gel towards the positive pole. The faster migration of XTENylated proteins than PASylated proteins has previously been observed by others [5].

The affinities of the five drug conjugates to HER2 were strong, in the low to sub-nanomolar range. However, Z_{HER2}, without any extension, has an even stronger affinity to HER2 (K_D 65 pM [9]). This shows that C-terminal extension of Z_{HER2} with an XTEN polypeptide, a PAS polypeptide, or an ABD leads to weaker affinity. Similar results have been reported by others, for example in an earlier study by Kubetzko et al. [27], which showed that conjugation of a large unstructured PEG polymer to a protein led to intra- and intermolecular blocking of target protein binding, giving a slower on-rate and consequently a weaker equilibrium dissociation constant. This phenomenon has also been observed when adding XTEN or PAS polypeptides to binding proteins [5].

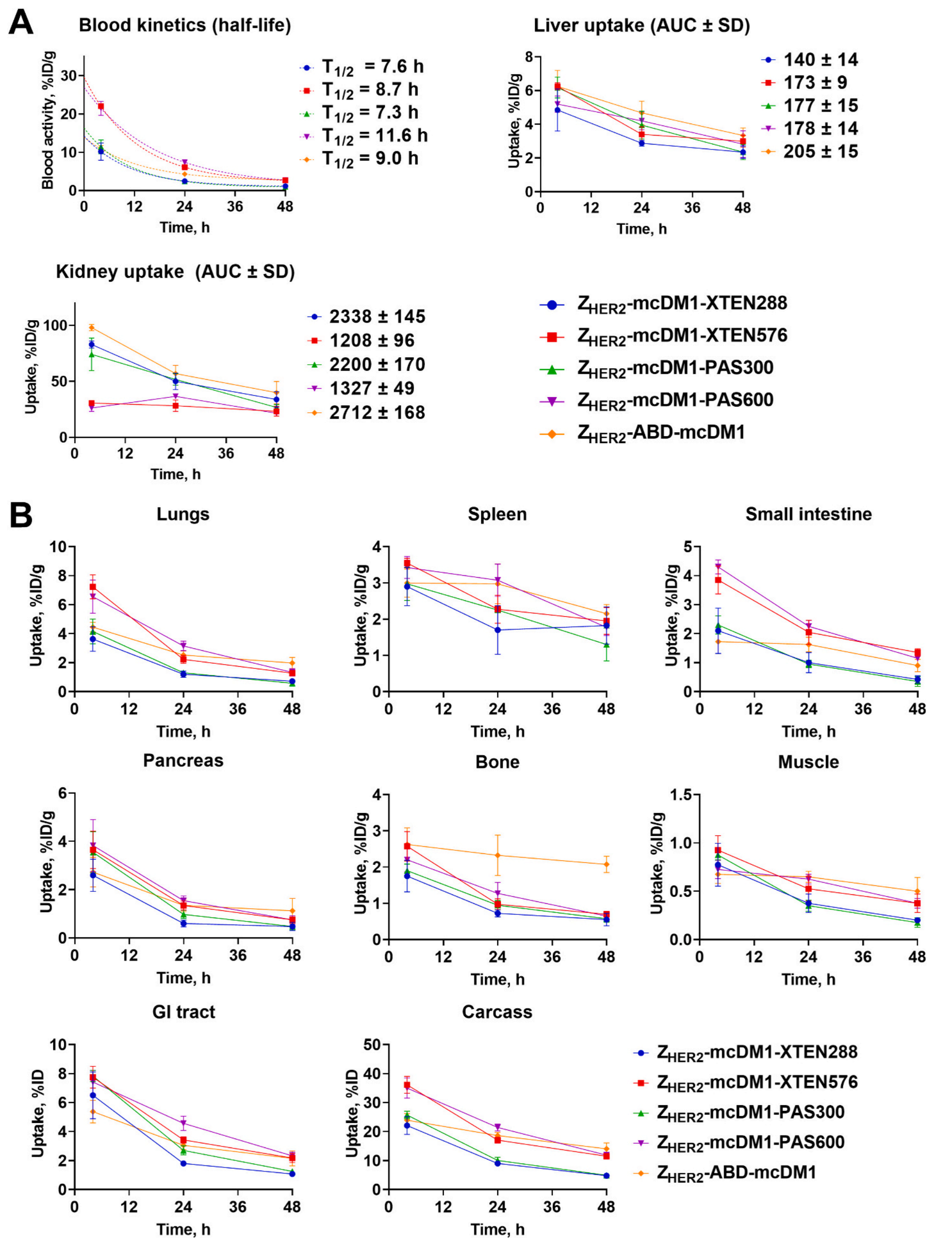

Fig. 5. Comparison of (A) blood kinetics, liver uptake, and kidney uptake of the [^{99m}Tc]Tc-labeled affibody-drug conjugates at 4 h, 24 h, and 48 h post-injection (p.i.) in CD-1 mice. The half-life in blood was calculated using a one-phase decay function. The area-under-the-curve is given to the right of each panel. Panel (B) shows the uptake in other organs. The uptake is displayed as %ID/g ± 1 SD, except for the GI tract and carcass, where it is shown as %ID/sample ± 1 SD.

The cytotoxic effect of the five drug conjugates was compared on HER2-positive cell lines. A strong and dose-dependent cytotoxic effect was observed for all fusion proteins, with IC_{50} values in the nanomolar range. There was a difference between the cell lines, where SKOV3 was more resistant to the cytotoxic action than the AU565 and SKBR3 cell lines. A similar pattern of SKOV3 resistance was observed in previous studies with affibody-drug conjugates [18,19]. Z_{HER2}-ABD-mcDM1 had a stronger cytotoxic effect on the SKBR3 cells than the other four drug conjugates. Compared to the non-half-life extended Z_{HER2}-mcDM1 the cytotoxicities of all five constructs were similar for the AU565 and the SKBR3 cell lines, but was weaker to the SKOV3 cell line [17].

The affinity measurements obtained from the SPR experiment evaluating binding to HER2 and from the LigandTracer experiments evaluating binding to living HER2-expressing SKOV3 cells correlated well. The PASylated conjugates generally had two-to-three times stronger K_D values than the XTENylated conjugates and had similar values to [^{99m}Tc]Tc-Z_{HER2}-ABD-mcDM1. It is of interest that the contribution of the high-affinity interaction (K_{D1}) for [^{99m}Tc]Tc-Z_{HER2}-ABD-mcDM1 was two times higher than for the PASylated and XTENylated conjugates on HER2-expressing SKOV3 cells, suggesting that it could provide better tumor targeting and retention *in vivo*.

An earlier study by Brandl et al., reporting on a DARPin expressed as a fusion with PAS or XTEN polypeptides, discussed that a possible electrostatic repulsion of the XTEN polypeptides by cellular membranes due to high negative charge might hinder their cellular uptake [5]. However, the results of the binding and internalization experiments in HER2-expressing SKOV3 and BT474 cells in this study show no major differences in internalization level between the PASylated and XTENylated conjugates (Fig. 4, Fig. S4). The internalization level of the PASylated and the XTENylated drug conjugates in this study was also comparable with the internalization of [^{99m}Tc]Tc-Z_{HER2}-ABD-mcDM1, with about 30% of the total added activity internalized in SKOV3 cells

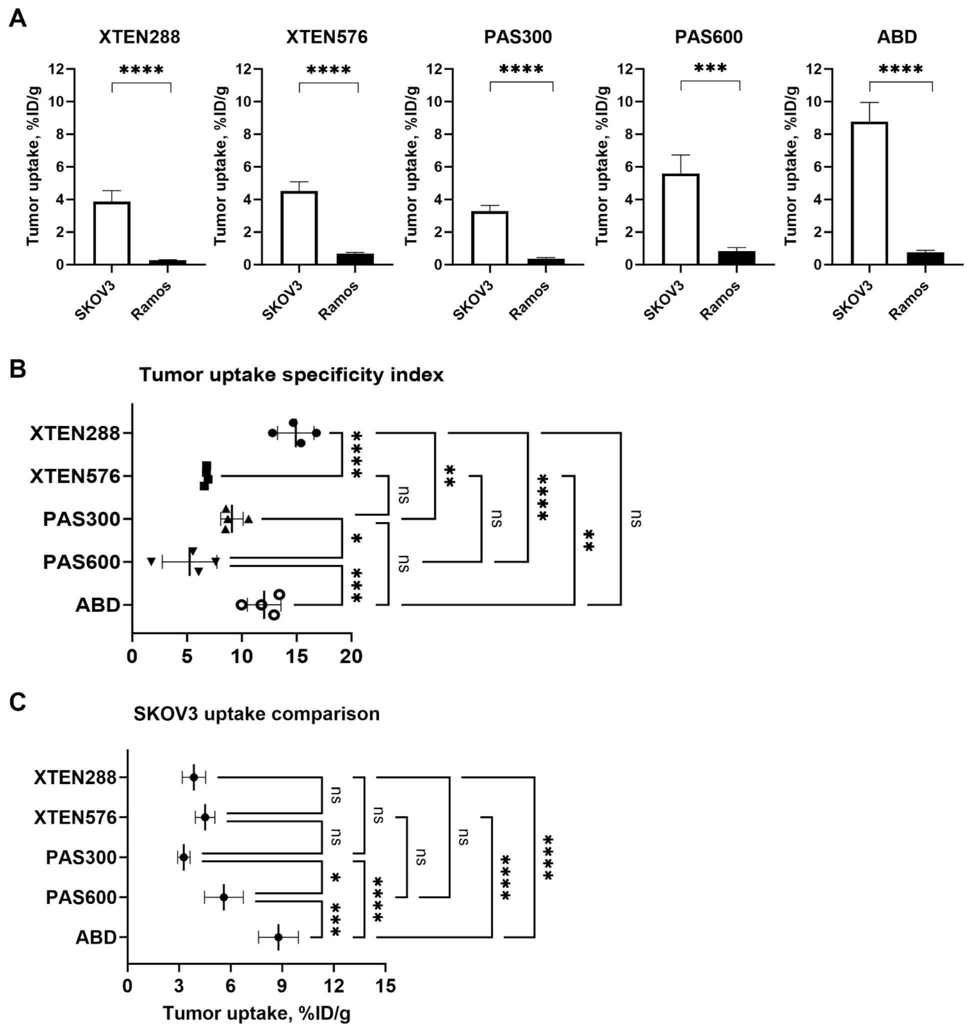

Fig. 6. Tumor targeting of [^{99m}Tc]Tc-labeled affibody-drug conjugates at 48 h p.i. in BALB/c nu/nu mice bearing HER2-expressing SKOV3 xenografts. (A) Targeting specificity comparison with HER2-negative Ramos xenografts. (B) Tumor uptake specificity index at 48 h p.i., calculated by dividing the value of uptake (%ID/g) of a conjugate in HER2-expressing SKOV3 xenografts by the value of its uptake in HER2-negative Ramos xenografts. (C) Side-by-side uptake comparison of the conjugates. Tumor uptake is shown as %ID/g ± 1 SD. Asterisks correspond to significant differences, where * corresponds to $p < 0.05$, *** corresponds to $p < 0.001$, and **** corresponds to $p < 0.0001$; ns – not significant.

and about 25% in BT474 cells by 24 h. This was slightly higher than earlier results found for a variant of $Z_{HER2:2891}$ ($Z_{HER2:342}$), which had an uptake by SKOV3 cells between 12% and 24% after 24 h [28]. This shows that elongation of Z_{HER2} with the XTEN or PAS polypeptides or the ABD does not negatively affect the internalization rate.

To quantitatively characterize the structure-property relationship of the affibody-based drug conjugates, site-specific radiolabeling of the N-terminal histidine-containing $(HE)_3$-tag with technetium-99m tricarbonyl, was used. This labeling method provides a radiolabel with residualizing properties that remains inside the cells following the binding and internalization processes. Therefore, it can accurately report the accumulation of a radiolabeled protein in an organ or tissue up until the studied time point. This method has been used in previous studies to develop affibody-based drug conjugates to select variants with optimized biodistribution profiles [18,19,29,30] and to characterize a DARPin fused with PAS or XTEN polypeptides [5]. The biodistribution of the PAS- or XTENylated drug conjugates in CD-1 mice showed that the half-life in blood correlated with their hydrodynamic radius, being shorter for the conjugates with a smaller hydrodynamic radius, and longer for the conjugates with a larger hydrodynamic radius. The kidney uptake was prevented by a large hydrodynamic radius where [^{99m}Tc]Tc-Z_{HER2}-mcDM1-XTEN576 and [^{99m}Tc]Tc-Z_{HER2}-mcDM1-PAS600 had two-fold lower kidney uptake compared to the other two. The half-life of [^{99m}Tc]Tc-Z_{HER2}-ABD-mcDM1 in blood was similar to that of [^{99m}Tc]Tc-Z_{HER2}-mcDM1-XTEN576. When Z_{HER2}-ABD-mcDM1 (14 kDa) is bound to serum albumin (66 kDa), its molecular weight increases to *ca.* 80 kDa, which is above the kidney filtration barrier and, therefore, prevents its rapid elimination from the blood. Moreover, its indirect interaction with FcRn though albumin should give it an extended half-life in addition to the extension by the increase in size, which the PASylated and XTENylated variants do not benefit from. However, the ABD-fused conjugate does not have any significantly longer *in vivo* half-life than the other four, and the FcRn-mediated extension, therefore, appears to be minor. The liver uptake of all five conjugates was similar and was thus not affected by the hydrodynamic radius.

The antibody-drug conjugate trastuzumab emtansine (T-DM1) also targets HER2, is loaded with DM1, and is used clinically for the treatment of breast cancer. A biodistribution study on ^{89}Zr-labeled T-DM1 showed uptake by BT474 xenografts (high HER2 expression) of 9.8 ± 1.1 %ID/g after 96 h [31]. This is similar to the uptake of [^{99m}Tc]Tc-Z_{HER2}-ABD-mcDM1 (8.8 ± 1.2 %ID/g) already after 24 h showing that Z_{HER2}-ABD-mcDM1 accumulates faster in the tumor than T-DM1. The biodistribution study on T-DM1 showed higher uptake in the liver compared to the kidneys, indicating a hepatobiliary excretion route, which is different from the predominantly renal excretion of the affibody-drug conjugates in this study. An unusually high uptake in the spleen was found for T-DM1. Even though the biodistribution studies are not exactly comparable since the affinities for HER2 are different, the drug loads are different, the time of analysis after injection is different, the radionuclides and chelators are different, it appears that the unspecific uptake by normal organs of T-DM1 and the drug conjugates in this study differs. It would be interesting to study if a combination of T-DM1 and a HER2-targeting affibody drug conjugate would increase the delivery of DM1 molecules to the tumor while keeping the uptake in normal organs low to minimize unwanted side effects.

The biodistribution measurement in tumor-bearing mice showed a similar tumor accumulation for [^{99m}Tc]Tc-Z_{HER2}-mcDM1-XTEN288, [^{99m}Tc]Tc-Z_{HER2}-mcDM1-PAS300, and [^{99m}Tc]Tc-Z_{HER2}-mcDM1-XTEN576. The accumulation of [^{99m}Tc]Tc-Z_{HER2}-mcDM1-PAS600 was 1.5-fold higher, which is likely due to its longest half-life in the blood. However, the highest absolute tumor uptake was found for [^{99m}Tc]Tc-Z_{HER2}-ABD-mcDM1 suggesting that the increase in hydrodynamic radius by PASylation and XTENylation hinders extravasation and tumor uptake.

The low uptake of the conjugates in the HER2-negative Ramos xenografts demonstrated a low level of passive targeting due to the enhanced permeability and retention (EPR) effect in tumors.

In conclusion, PASylation and XTENylation of the affibody-based drug conjugate appears to be less efficient strategies for tumor-targeted drug delivery than its fusion with ABD since the PAS and XTEN polypeptides provided lower values of tumor uptake with similar or higher accumulation in normal organs and tissues, resulting in lower tumor-to-organ ratios.

CRediT authorship contribution statement

Jie Zhang: Writing – original draft, Validation, Investigation, Formal analysis, Data curation. **Vitalina Bodenko:** Methodology, Investigation, Formal analysis, Data curation. **Maria Larkina:** Methodology, Investigation, Formal analysis, Data curation. **Ekaterina Bezverkhniaia:** Methodology, Investigation, Formal analysis, Data curation. **Tianqi Xu:** Writing – original draft, Methodology, Investigation, Formal analysis, Data curation. **Yunqi Liao:** Investigation, Formal analysis. **Ayman Abouzayed:** Methodology, Investigation, Formal analysis, Data curation. **Evgenii Plotnikov:** Methodology, Investigation, Formal analysis, Data curation. **Maria Tretyakova:** Writing – review & editing, Methodology, Investigation, Formal analysis, Data curation. **Feruza Yuldasheva:** Writing – review & editing, Methodology, Investigation, Formal analysis. **Mikhail V. Belousov:** Writing – review & editing, Supervision, Resources, Investigation, Funding acquisition, Formal analysis. **Anna Orlova:** Writing – review & editing, Supervision, Resources, Investigation, Formal analysis. **Vladimir Tolmachev:** Writing – review & editing, Writing – original draft, Supervision, Resources, Project administration, Methodology, Investigation, Data curation, Conceptualization. **Torbjörn Gräslund:** Writing – review & editing, Writing – original draft, Supervision, Resources, Project administration, Methodology, Funding acquisition, Conceptualization. **Anzhelika Vorobyeva:** Writing – review & editing, Writing – original draft, Supervision, Resources, Project administration, Methodology, Investigation, Formal analysis, Conceptualization.

Declaration of competing interest

Anna Orlova and Vladimir Tolmachev own shares in Affibody Medical AB (Solna, Sweden), and Zytox Therapeutics AB (Stockholm, Sweden). Torbjörn Gräslund, and Anzhelika Vorobyeva owns shares in Zytox Therapeutics AB. The other authors declare no conflict of interest.

Data availability

Data will be made available upon request.

Acknowledgments

This research was funded by the Swedish Agency for Innovation VINNOVA (2019/00104), VR 2019-00994 (V. T.), VR 2022-01519 (A. V.) and the Swedish Cancer Society Cancerfonden (CAN 21 1861 Pj (T. G.); 20 0181 P (A.V.); 20 0893 Pj (A.V.); 23 0650 JIA (A.V.); 20 0815 PjF (A.O.)).

Appendix A. Supplementary data

Supplementary data to this article can be found online at https://doi.org/10.1016/j.jconrel.2024.04.051.

References

[1] R. Zaman, et al., Current strategies in extending half-lives of therapeutic proteins, J. Control. Release 301 (2019) 176–189.
[2] J.P. Martins, P.J. Kennedy, H.A. Santos, C. Barrias, B. Sarmento, A comprehensive review of the neonatal fc receptor and its application in drug delivery, Pharmacol. Ther. 161 (2016) 22–39.
[3] M. Schlapschy, et al., PASylation: a biological alternative to PEGylation for extending the plasma half-life of pharmaceutically active proteins, Protein Eng. Des. Sel. 26 (2013) 489–501.
[4] V. Schellenberger, et al., A recombinant polypeptide extends the in vivo half-life of peptides and proteins in a tunable manner, Nat. Biotechnol. 27 (2009) 1186–1190.
[5] F. Brandl, et al., Influence of size and charge of unstructured polypeptides on pharmacokinetics and biodistribution of targeted fusion proteins, J. Control. Release 307 (2019) 379–392.
[6] S. Ståhl, et al., Affibody molecules in biotechnological and medical applications, Trends Biotechnol. 35 (2017) 691–712.
[7] A. Orlova, et al., Tumor imaging using a picomolar affinity HER2 binding Affibody molecule, Cancer Res. 66 (2006) 4339–4348.
[8] H.J. Burstein, The distinctive nature of HER2-positive breast cancers, N. Engl. J. Med. 535 (2005) 1652–1654.
[9] J. Feldwisch, et al., Design of an optimized scaffold for affibody molecules, J. Mol. Biol. 398 (2010) 232–247.
[10] O. Bragina, et al., Phase I clinical evaluation of 99mTc-labeled Affibody molecule for imaging HER2 expression in breast cancer, Theranostics 13 (2023) 4858–4871.
[11] A. Alhuseinalkhudhur, et al., Human epidermal growth factor receptor 2-targeting [68Ga]Ga-ABY-025 PET/CT predicts early metabolic response in metastatic breast Cancer, J. Nucl. Med. 64 (2023) 1364–1370.
[12] J. Sörensen, et al., First-in-human molecular imaging of HER2 expression in breast cancer metastases using the 111In-ABY-025 affibody molecule, J. Nucl. Med. 55 (2014) 730–735.
[13] J. Sörensen, et al., Measuring HER2-receptor expression in metastatic breast cancer using [68Ga]ABY-025 Affibody PET/CT, Theranostics 6 (2016) 262–271.
[14] A. Jonsson, J. Dogan, N. Herne, L. Abrahmsén, P.Å. Nygren, Engineering of a femtomolar affinity binding protein to human serum albumin, Protein Eng. Des. Sel. 21 (2008) 515–527.
[15] S. Verma, et al., Trastuzumab emtansine for HER2-positive advanced breast cancer, N. Engl. J. Med. 367 (2012) 1783–1791.
[16] S.O. Doronina, et al., Enhanced activity of monomethylauristatin F through monoclonal antibody delivery: effects of linker technology on efficacy and toxicity, Bioconjug. Chem. 17 (2006) 114–124.
[17] M. Altai, et al., Affibody-derived drug conjugates: potent cytotoxic molecules for treatment of HER2 over-expressing tumors, J. Control. Release 288 (2018) 84–95.
[18] T. Xu, et al., Drug conjugates based on a monovalent affibody targeting vector can efficiently eradicate HER2 positive human tumors in an experimental mouse model, Cancers (Basel) 13 (2021) 85.
[19] W. Yin, et al., Comparison of HER2-targeted affibody conjugates loaded with auristatin- and maytansine-derived drugs, J. Control. Release 355 (2023) 515–527.
[20] T. Xu, et al., Effect of inter-domain linker composition on biodistribution of ABD-fused Affibody-drug conjugates targeting HER2, Pharmaceutics 14 (2022).
[21] R. Waibel, et al., Stable one-step technetium-99m labeling of his-tagged recombinant proteins with a novel Tc(I)-carbonyl complex, Nat. Biotechnol. 17 (1999) 897–901.
[22] V. Tolmachev, et al., HEHEHE-tagged affibody molecule may be purified by IMAC, is conveniently labeled with [99mTc(CO)3]+, and shows improved biodistribution with reduced hepatic radioactivity accumulation, Bioconjug. Chem. 21 (2010) 2013–2022.
[23] H. Ding, et al., Incorporation of a hydrophilic spacer reduces hepatic uptake of HER2-targeting Affibody–DM1 drug conjugates, Cancers (Basel) 11 (2019) 1168–1187.
[24] H. Wållberg, A. Orlova, Slow internalization of anti-HER2 synthetic affibody monomer 111In-DOTA-ZHER2:342-pep2: implications for development of labeled tracers, Cancer Biother. Radiopharm. 23 (2008) 435–442.

[25] S. Ahlgren, et al., Targeting of HER2-expressing tumors using 111In-ABY-025, a second-generation Affibody molecule with a fundamentally reengineered scaffold, J. Nucl. Med. 51 (2010) 1131–1138.
[26] H. Liu, et al., Potent and specific fusion toxins consisting of a HER2-binding, ABD-derived affinity protein, fused to truncated versions of Pseudomonas exotoxin a, Int. J. Oncol. 55 (2019) 309–319.
[27] S. Kubetzko, C.A. Sarkar, A. Plückthun, Protein PEGylation decreases observed target association rates via a dual blocking mechanism, Mol. Pharmacol. 68 (2005), 1439 LP – 1454.
[28] H. Wållberg, et al., Molecular design and optimization of 99mTc-labeled recombinant affibody molecules improves their biodistribution and imaging properties, J. Nucl. Med. 52 (2011) 461–469.
[29] W. Yin, et al., The influence of domain permutations of an albumin-binding domain-fused her2-targeting affibody-based drug conjugate on tumor cell proliferation and therapy efficacy, Pharmaceutics 13 (2021) 1974.
[30] H. Ding, et al., Affibody-derived drug conjugates targeting HER2: effect of drug load on cytotoxicity and biodistribution, Pharmaceutics 13 (2021) 430.
[31] N. Al-saden, Z. Cai, R.M. Reilly, Tumor uptake and tumor/blood ratios for 89Zr-DFO-trastuzumab-DM1 on microPET/CT images in NOD/SCID mice with human breast cancer xenografts are directly correlated with HER2 expression and response to trastuzumab-DM1, Nucl. Med. Biol. 67 (2018) 43–51.